Defence Science Journal, Vol. 58, No. 3, May 2008, pp. 327-337

Numerical Analysis of Integrated Liquid Ramjet Engine

G. Raja Singh Thangadurai[1], B.S. Subhash Chandran[1], V. Babu[2], and T. Sundararajan[2]

[1]*Defence Research & Development Laboratory, Hyderabad-500 058*
[2]*Indian Institute of Technology Madras, Chennai-600 036*

ABSTRACT

The numerical simulation of an integrated, liquid-fuelled ramjet engine comprising supersonic air intake, subsonic combustor and a convergent-divergent nozzle has been carried out and the results are discussed in this paper. These results include cold flow studies, heat addition in the combustor and full engine analysis with coupled simulation of supersonic air-intake and combustion chamber along with the nozzle. Overall ramjet operation depends on the performance of the air intake and the combustion chamber. The coupling phenomena are very dominant and performance of air intake is affected vastly by the combustor operation and vice versa. In this paper, a numerical analysis of integrated liquid ramjet engine considering coupling phenomena between various sub-systems viz., air intake, combustor and nozzle has been reported.

Keywords: Ramjet engine, air intake, combustor, numerical simulation, internal flow, air/fuel ratio

1. INTRODUCTION

Ramjet engines are lighter than rockets since they utilise ambient air as the oxidiser for combustion of fuel. The major constituents of a liquid ramjet engine are air-intake, combustion chamber, and nozzle. The full engine simulation is useful for understanding the various important aspects of ramjet internal flows that include shockwave/boundary layer interactions, inlet/combustor coupling, flame holding and spreading, and combustion dynamics. Thomas[1] presented documented facts about the current status of ramjets and ramjet technology and concluded that ramjets possess the unique ability to provide continuous thrust, sustained high supersonic speed and high specific impulse. Hebrard[2], *et al.* employed a combined approach using experiments in isothermal conditions and simple computation models to study the global performances of various ramjets. Calzone[3] carried out a study of the international developments on missile ramjet propulsion. The choice and techniques to be used during the design of a liquid-fuelled ramjet engine were described in detail by Cazin and Laurent [4].The specific features of the constituents of a ramjet engine such as the air supply system, fuel supply system, combustion chamber and the nozzle, were discussed. Conway and Johansson[5] dealt with the development and validation of a methodology for simulation of ramjet -powered missiles using computational fluid dynamics (CFD). Simultaneous calculations of the internal and external flows were carried out by coupling a quasi one- dimensional ramjet engine model with a CFD solver. A thermally perfect gas assumption was adopted to enable accurate modelling of the hot nozzle gas flow. Tip to tail calculations were carried out on two ramjet-powered vehicles

Received 24 January 2006, revised 19 June 2007

and results were compared with available and wind tunnel data. Sung[6], *et al*. numerically analysed an entire ramjet engine to understand the combustion dynamic characteristics of an integrated rocket ramjet system.Various physical processes were investigated systematically, including flame propagation, flame dynamics, turbulent flame evolution, terminal shock train, modal analysis of the system, and interaction mechanism between the oscillating shockwave in the diffuser and pressure wave resulting from heat release, using spectral analysis. Gaiddon and Knight[7] used an automated optimisation loop based on CFD tools for improving the flight performance of a ramjet-powered missile. For each point of the mission (acceleration, cruise, and manoeuvre) the best inlet shape was determined. Multi-objective optimisations were then performed to obtain the best set of shapes satisfying the whole mission., The coupling phenomena between the various subsystems of a liquid ramjet engine, namely the air-intake, combustor, and nozzle have been investigated in the present study.

2. SIMULATION OF A RAMJET ENGINE

The performance of a ramjet engine depends on the efficient operation of both the air intake and combustion chamber. Since the operations of these subsystems are inter-dependent, there is a requirement to carry out the simulation of a complete ramjet engine in totality to analyse its realistic performance characteristics. Complete simulation also helps in choosing the proper location and size of air inlets as well as the combustor geometry to obtain the best overall engine performance. However, a very important factor that needs deep consideration is the interaction between the intake, combustor, and the nozzle flows. For example, in sub-critical condition, the unattached shock may lead to air spillage, which could result in poor combustion and loss of thrust. On the other hand, in super-critical condition during which the shock train moves into the diffuser, pressure recovery may be poor, again resulting in lower propulsion efficiency. The locations of the shock as well as the shock reflections are affected not only by the geometries of the intake but also by the amount of heat release in the combustor. The extent of flow acceleration in the nozzle depends on both the stagnation pressure and stagnation temperature conditions achieved in the combustor section. Thus, a comprehensive understanding of air intake-combustor-nozzle interactions requires a solution obtained through integrated ramjet simulation.

The full engine simulation is useful in understanding the various important aspects of ramjet internal flows that include shockwave/boundary layer interactions, inlet/combustor coupling, flame holding and spreading, and combustion dynamics. Since the focus of this study is on the coupling phenomena between the various subsystems, a simple axi-symmetric engine geometry (consisting of axi-symmetric intake, axi-symmetric combustor and axi-symmetric nozzle) has been considered (Fig. 1). In order to achieve aerodynamic flame holding in the combustor, a sudden expansion has been introduced at the end of the intake. Fuel is injected close to the re-circulation zone, which occurs after the sudden expansion.

In order to clearly highlight the flow phenomena due to geometry and the effects of spray mixing as well heat release by combustion, the simulation of the complete ramjet engine has been carried out in the following three stages:

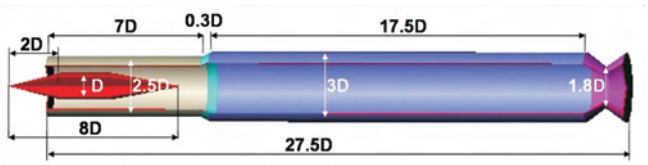

Figure 1. Ramjet engine with axi-symmetric intake, combustor and nozzle.

(i) Simulation with cold air flow,

(ii) Simulation with equivalent heat addition at the combustor wall, and

(iii) Simulation with fuel spray and combustion in the combustor.

The main parameters which are varied in the full simulation studies are the flight Mach number and the air/fuel ratio.

3. COLD FLOW STUDIES IN A RAMJET ENGINE

To simulate the entire ramjet engine, a cylindrical combustion chamber with a convergent divergent

nozzle is attached to the exit section of the air intake. The grid employed for simulation studies is shown in Fig. 2. This arrangement is useful in analysing the ramjet engine in totality. For the numerical calculations the system of governing differential equations for a steady, compressible and turbulent flow have been solved using the commercial software FLUENT with appropriate boundary conditions. On the left hand side (inlet) boundary and on the top and bottom boundaries, the free stream temperature, pressure and Mach number conditions have been imposed. On the walls of the engine and on the centre body, adiabatic conditions along with standard wall functions have been prescribed. On the right boundary, supersonic outlet conditions have been prescribed for both internal and external flow streams. All the flow variables including pressure are determined from the interior domain by extrapolation.

The turbulence model used in the present simulation study is the standard k-ε model which employs two partial differential equations to estimate the velocity and length scales of turbulence. The standard wall functions described by Launder and Spalding[8] are used in the present calculations. Numerical simulations were carried out using three different grid sizes with 100 x 100, 150 x 150, and 200 x 200 nodes in the axial and radial directions to obtain solutions for cold air flow through the engine. Based on grid sensitivity analysis, grid size of 200 x 200 has been chosen for all calculations. The predicted static pressure and Mach contours for cold flow analysis of a typical case are shown in Figs 3 and 4 respectively. With the enlarged combustion chamber the terminal normal shock moves further downstream inside the air duct. The oblique shocks attached to the fore body, tip of the cowl and also near the sudden expansion section in the external flow, are clearly seen in the static pressure and Mach contours. It is interesting to note that the peak pressure value is achieved only just before the nozzle section.

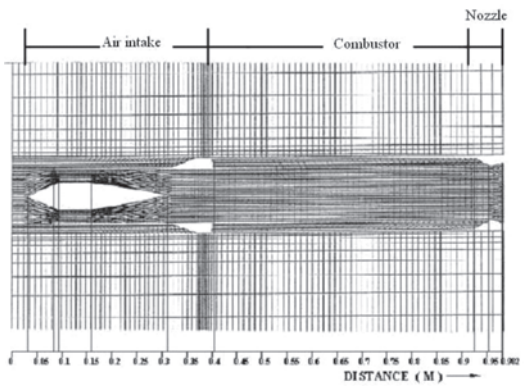

Figure 2. Grid for integrated engine.

At a higher Mach number, the static pressure recovery is also greater as expected. A closer scrutiny of the Mach number contours reveals reflected oblique shock patterns in the intake region. Expansion of the flow (compressed by shock in the intake) is observed across the nozzle.Stream

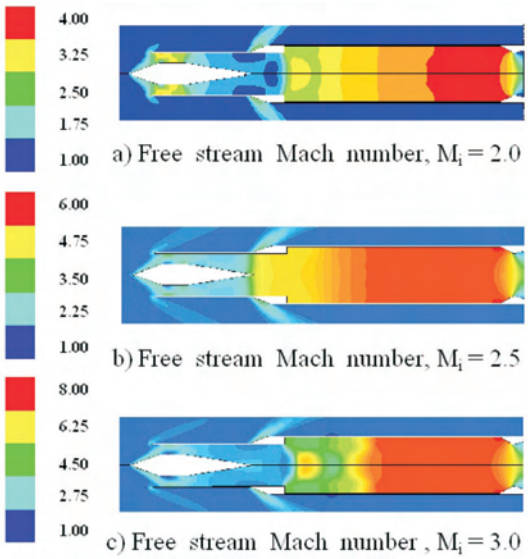

Figure 3. Static pressure (bar) contours for cold air flow.

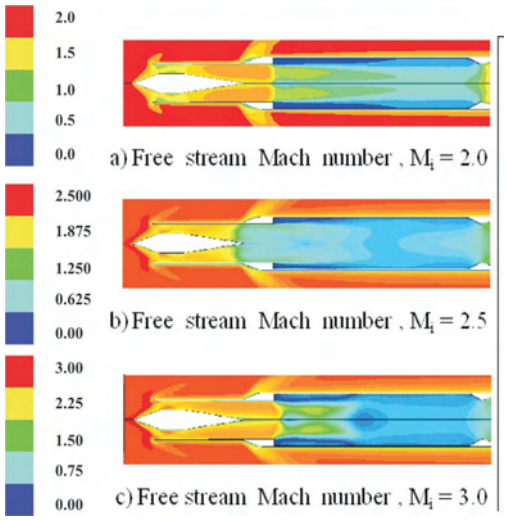

Figure 4. Mach contours for cold air flow.

function contours are shown in Fig. 5. A re-circulation zone is observed where there is sudden enlargement in the combustion chamber area. The size of the re-circulation eddy is seen to increase with Mach number.

4. SIMULATION WITH HEAT ADDITION IN THE COMBUSTOR

For the simulation of hot flow in a ramjet engine, the thermal input for a typical ramjet engine was distributed over the combustion chamber wall as a uniform heat flux. Steady state combustion of the combustible mixture in a ramjet combustor for a fixed set of flow variables generates a constant heat input. Uniform heat flux distributed over the cylindrical combustion chamber wall produces a constant heat input. The heat input is arrived at by considering the following nominal conditions that prevail in a typical practical ramjet engine: Air/fuel ratio = 15; air mass flow rate = 7 kg/s; fuel flow rate = 0.4667 kg/s. Kerosene (JP-8) is used as the fuel for simulation studies. For the above conditions the heat input works out to be 10 MW.

The parametric study has been carried out for heat inputs of 10 MW, 12 MW and 15 MW. As in the case of cold flow simulation, grid size of 200 x 200 has been chosen for carrying out calculations with heat addition in the combustion chamber. For a given geometry, at a fixed free stream Mach number and altitude of operation, the mass flow rate through the intake is constant. This mass flow rate (for a given throat area) is proportional to $p_o/T_o^{1/2}$. When the stagnation temperature is increased due to heat addition in the combustion chamber, the mass flow rate through the combustor has to be decreased. To achieve this, the normal shock moves upstream where the Mach number is higher. This results in increased loss of stagnation pressure thereby reducing the mass flow rate. With heat addition, the terminal normal shock moves upstream and is located near the narrowest cross section of the air intake. The contours of static pressure and Mach number for this condition shown in Figs 6 and 7 corroborate this observation. Due to the forward movement of the terminal shock, the peak pressure value is attained in the rear part of the intake zone itself, for free stream Mach numbers of 2.0 and 2.5. For a free stream Mach number of 3.0 also, most of the pressure recovery occurs in the intake, although a small pressure rise is seen in the combustor zone.

However, a closer scrutiny of the pressure values indicated a small drop (Fig. 6) in the rear part of the combustor, which can be attributed to the effect of heat addition in the constant area section. Thus, the Rayleigh flow in the constant area combustion chamber also has been predicted well and the pressure drop across the combustor matched well with the predictions of the corresponding

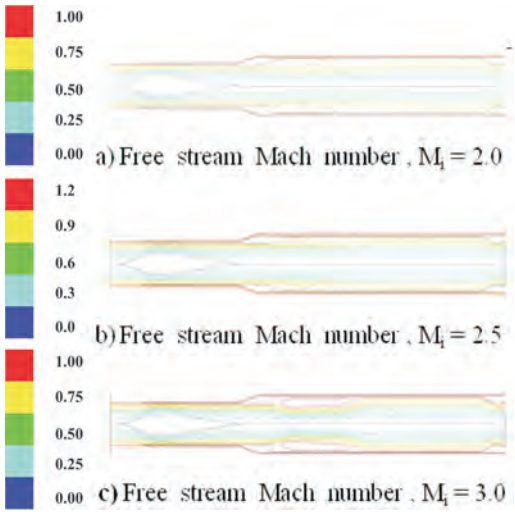

Figure 5. Stream function (m^3/s) contours for cold air flow.

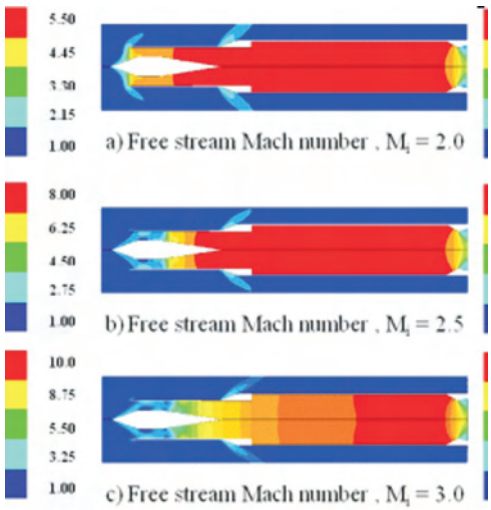

Figure 6. Static pressure (bar) contours for air flow with heat addition (12 MW) in the combustor.

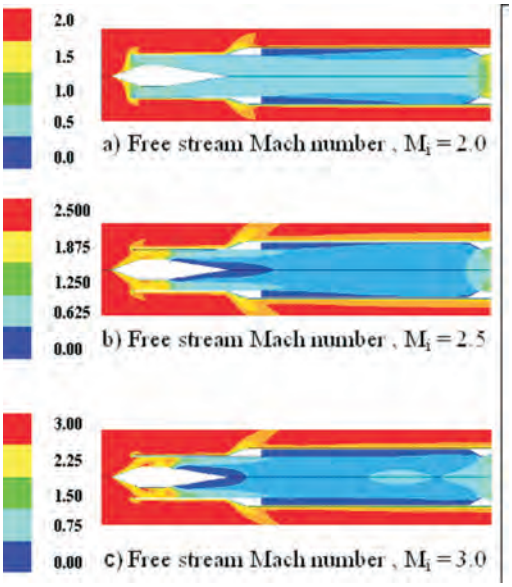

Figure 7. Mach contours for air flow with heat addition (12 MW) in the combustor.

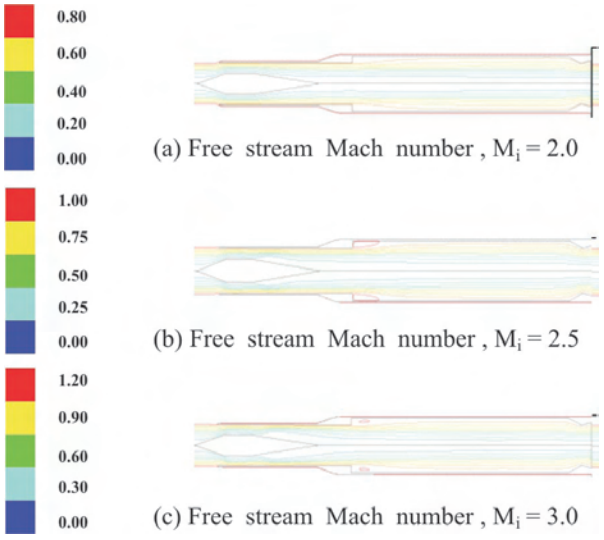

Figure 8. Stream function (m^3/s) contours for air flow with heat addition (12 MW) in the combustor.

one-dimensional analysis. The peak pressure values attained for the cases with heat addition are higher than the corresponding values shown for cold flow case (Fig. 3), for each Mach number considered. Thus, it is evident that the shock locations and the shock compression process are intimately coupled with the heat addition due to combustion in the combustion chamber. The Mach number contours depicted in Fig. 7 illustrates that the terminal normal shock (corresponding to the transition from M>1 to M<1) is located at the entry section for the free stream Mach number of 2.0, while the terminal shock location moves to the constant area section of the intake for M = 2.5 and M = 3.0. The streamline contours in the combustion chamber portion are shown in Fig. 8. It is seen that re-circulatory eddies are present near the sudden expansion for the case with heat addition also.

Moreover, flow separation is observed at the end of the constant area portion of the intake for M = 2.5 and M = 3.0. The static pressure distribution along the centre body outer surface and axis for the cases, with and without thermal input in the combustion chamber inner wall, are shown in Fig. 9. It is evident that heat addition significantly increases the static pressure recovery for the given flow geometry. However, for a given free stream Mach number as the heat addition is increased, the rate of increase in static pressure rise becomes less. These trends can be attributed to the changes in the shock locations and their strength due to heat addition. In Fig. 10, the effects of heat addition on the Mach number distribution in the axial direction are shown. It is evident that the flow decelerates from supersonic to subsonic condition because of the terminal normal shock. Beyond this shock, in the combustor section, slight flow acceleration is seen even before the nozzle portion. For the cold flow case, it is clear that the terminal shock occurs very much inside the combustor region. The axial variation in static temperature is depicted in Fig. 11 for different free stream Mach numbers.

Static temperature increases across the oblique shock and the terminal normal shock in the intake region. The Mach number continues to increase in the combustor region due to heat addition.The captured air mass flow rate is different for different Mach numbers and hence temperature rise $(\Delta T = \dot{Q} / \dot{m}\, c_p)$ due to heat addition varies with Mach number.

5. SIMULATION WITH COMBUSTION IN THE COMBUSTOR

Simulation studies were also carried out for a full liquid ramjet engine comprising all the constituent assemblies such as airintake, fuel injector, combustion chamber and nozzle. The exact operation has been simulated by injecting fuel in the combustor, immediately

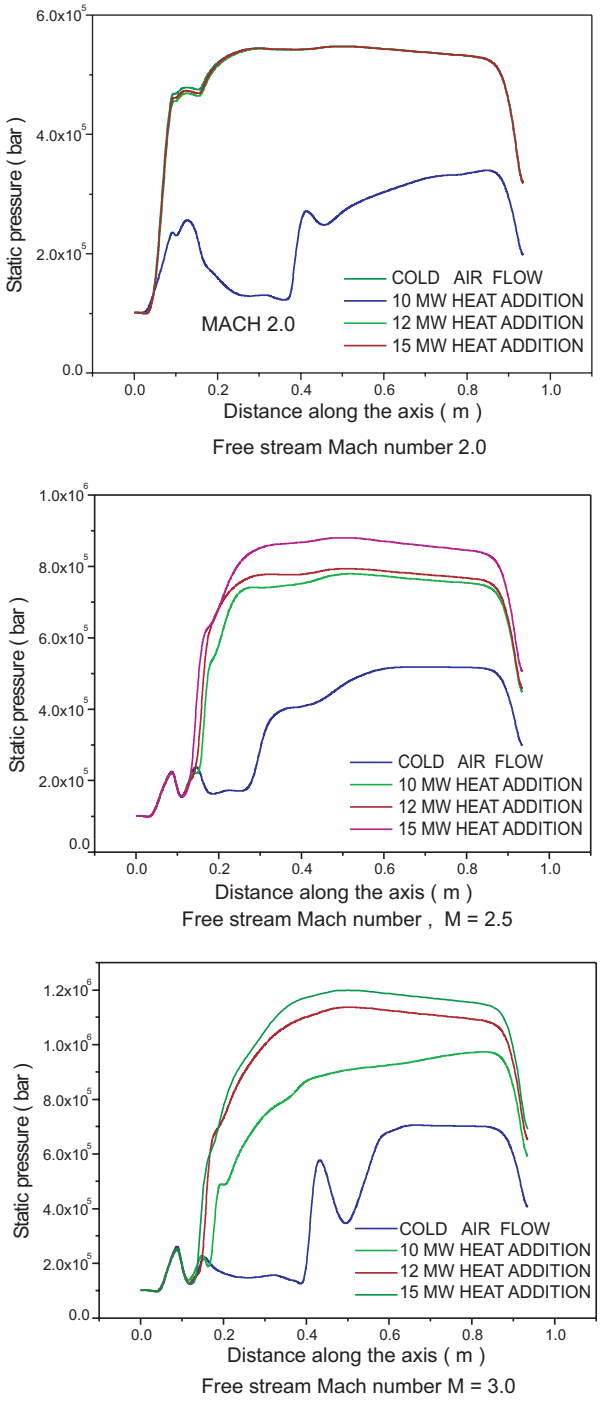

Figure 9. Effect of heat addition on the static pressure distribution along the axis.

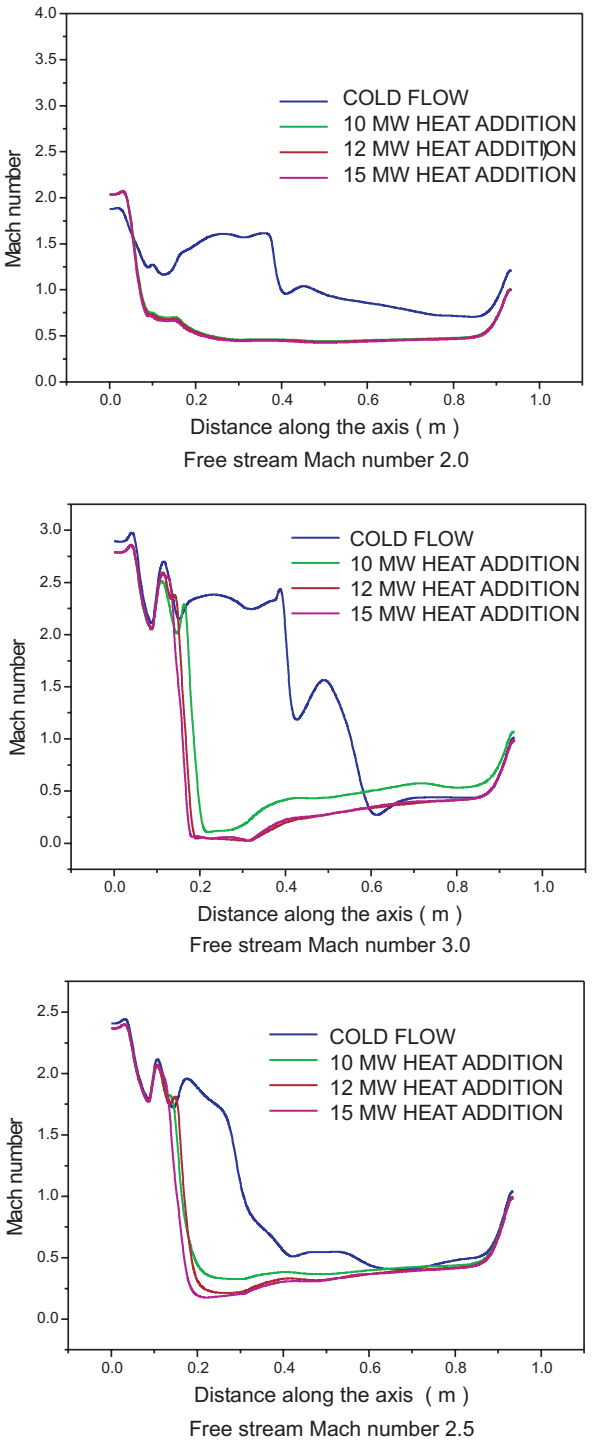

Figure 10. Effect of heat addition on the Mach number distribution along the axis.

after the sudden expansion section. The computational domain is given in Fig.12

The effect of free stream Mach number and air/fuel ratio (A/F) on the ramjet engine performance have been studied in detail. Full engine simulations have been carried out with three different grids having 11090, 22080 and 44350 cells. Refinement of the grid has been carried out at the location where steep gradients of temperature and pressure are seen. All the

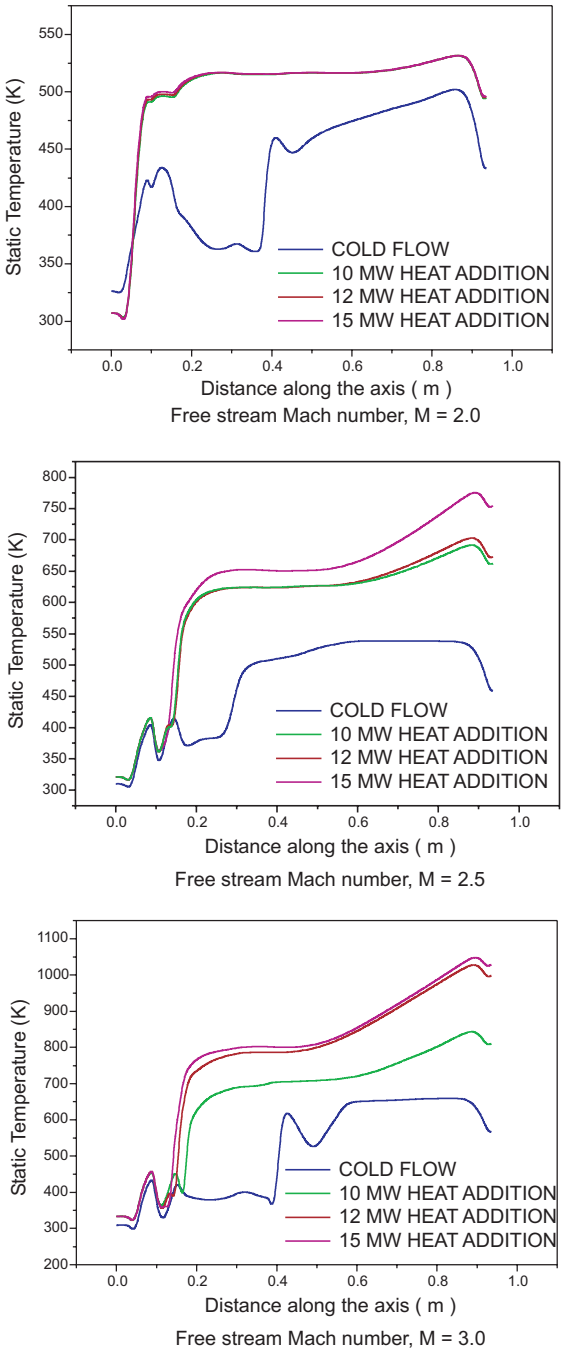

Figure 11. Effect of heat addition on the static temperature distribution along the axis.

results reported here have been obtained on the finest grid, i.e., with 44350 cells.

5.1 Effect of Free Stream Mach Number

The contours of Mach number and static temperature for inlet Mach numbers of 2.0, 2.5 and 3.0 are shown in Figs 13 and 14 respectively. The ir/fuel ratio for this case was 17. Mach number contours for inlet Mach number equal to 2 (Fig. 13) indicate that the shock train is located outside the intake, which results in spillage of air flow. For M_i = 2.5, the spillage is reduced and the terminal normal shock is located at the entry section. For M_i = 3.0, the shock train moves into the intake; here, the feature of reflected oblique shocks culminating in a terminal shock is clearly seen.These three cases of M_i = 2.0, 2.5 and 3.0 correspond to the sub-critical, critical (approximately) and super-critical operation of the engine respectively. From the temperature contours (Fig. 14) it is seen that combustion primarily occurs close to the wall, near the sudden expansion section.The re-circulatory region and boundary layer close to the wall aid in flame stabilisation. In this study, the conserved-scalar approach based on the fast-chemistry assumption is adopted to account for the turbulence-combustion interaction. The maximum temperature attained is highest for M_i = 3.0, since the shock compression process results in a higher pre-ignition temperature for this case because of stronger shocks.

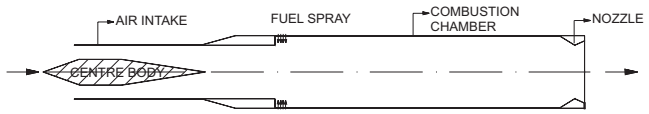

Figure 12. Computational domain.

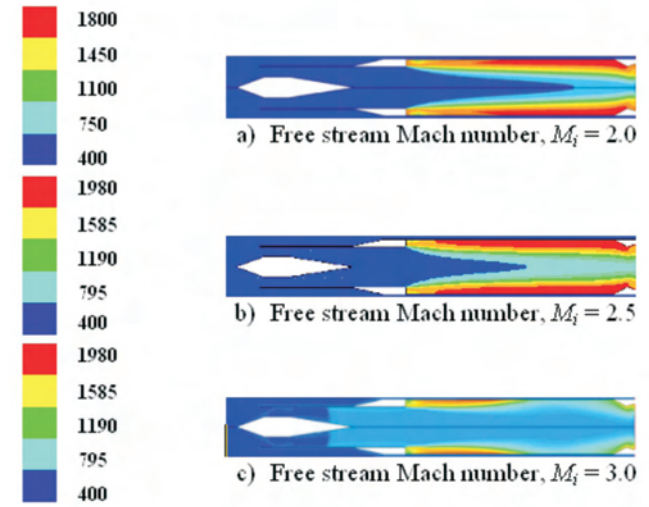

Figure 13. Mach contours for air/fuel ratio = 17.

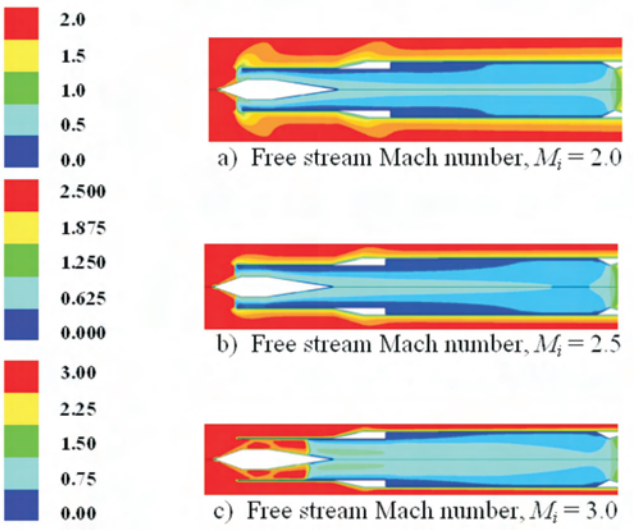

Figure 14. Temperature (K) contours for air/fuel ratio.

Although maximum temperature is higher, the average temperature is lower for M_i = 3.0 due to larger mass flow rate. In Fig. 15, the fuel mass fraction contours are plotted. It is clear that fuel disperses more at M_i = 2.0 as compared to the cases of M_i = 2.5 and 3.0. Therefore, the combustion zone is larger for M_i = 2.0. The static pressure, static temperature and Mach number variation along the surface of the centre body and axis are shown in Figs 16, 17 and 18 respectively. The static pressure and temperature increase across the terminal normal

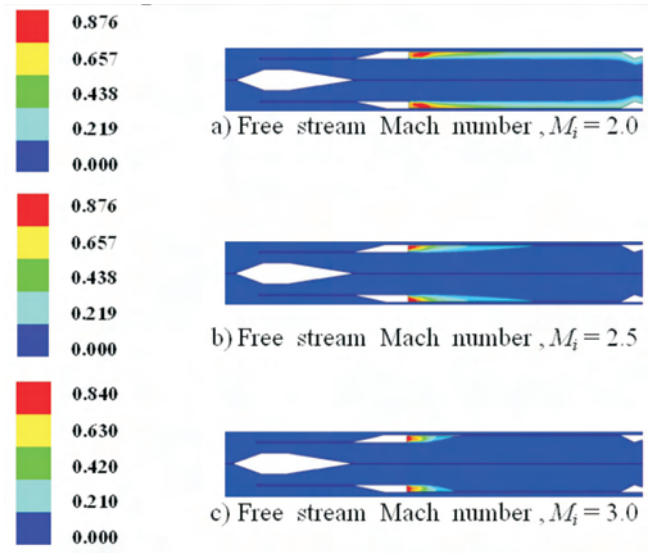

Figure 15. Mass fraction contours of fuel for air/fuel ratio = 17.

shock, while the Mach number decreases to subsonic values. In fact, for M_i = 3.0, features such as flow deceleration at the first shock, re-acceleration immediately after the shock and subsequent transition to subsonic flow at the terminal normal shock can be clearly discerned. Also, at M_i = 3.0, combustion phenomenon does not penetrate up to the axis and hence temperature rise is marginal along the axis.

5.2 Effect of Air/Fuel Ratio

Results for an air fuel ratio of 30 are presented in Figs. 19 and 20. Compared with the previous case for which the air/fuel ratio was 17, significant changes can now be seen. For example, the Mach number contours show that the ramjet operation

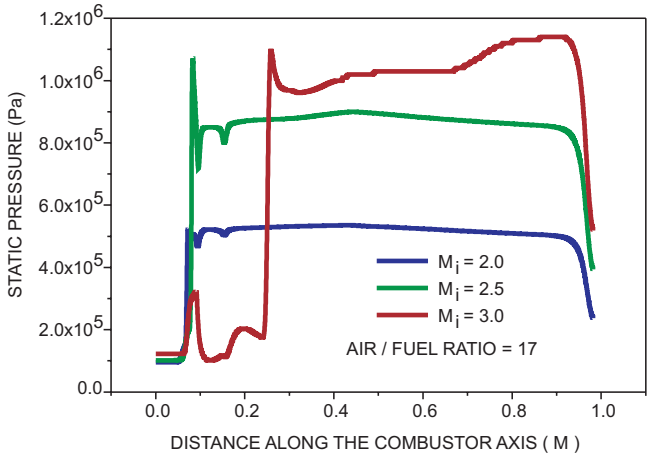

Figure 16. Variation of static pressure alng the surface and axis of the centre body.

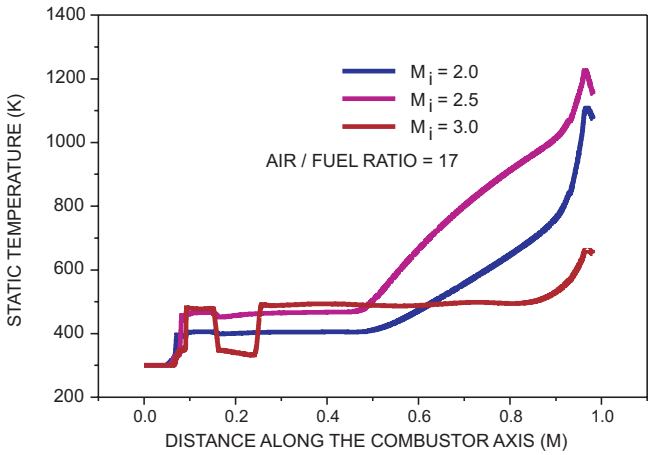

Figure 17. Variation of temperature along the surface and axis of the centre body.

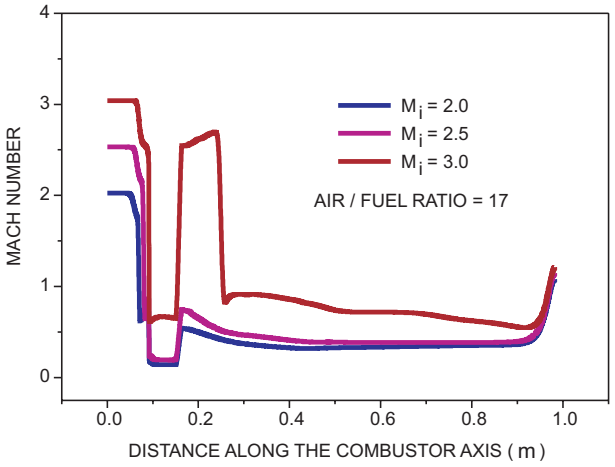

Figure 18. Mach number variation along the surface and axis of the centre body.

becomes super-critical (shocks moves within the intake) even for $M_i = 2.5$. Also, the extent of spillage decreases for $M_i = 2.0$. In addition, the inward movement of the shock system, results in higher temperature values for M_i = 2.5 and 3.0. However, most of the features of the combustion zone such as fuel dispersion, (Fig. 21) are similar to the corresponding predictions for A/F = 17. In Figs 22 - 24, the centre line variations of static pressure, static temperature and Mach number also indicate the slight shift in the location of the normal shock at M_i = 2.5. Consequently, the flow and pressure recovery are modified. For inlet Mach number of 2.5, the peak temperature observed for an A/F of 17 is 1980 K as compared to 1920 K for

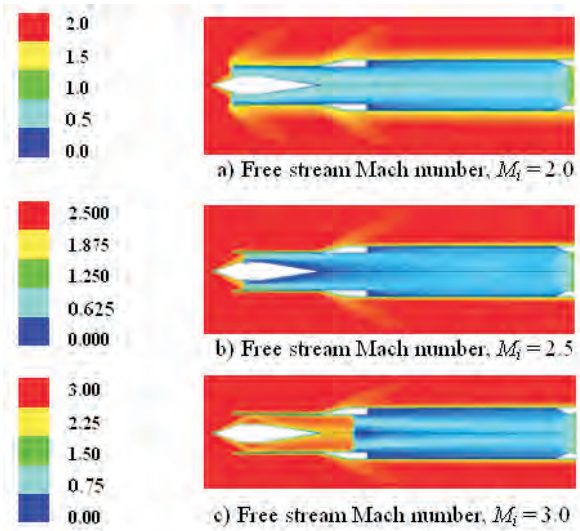

Figure 19. Mach contours for air/fuel ratio= 30.

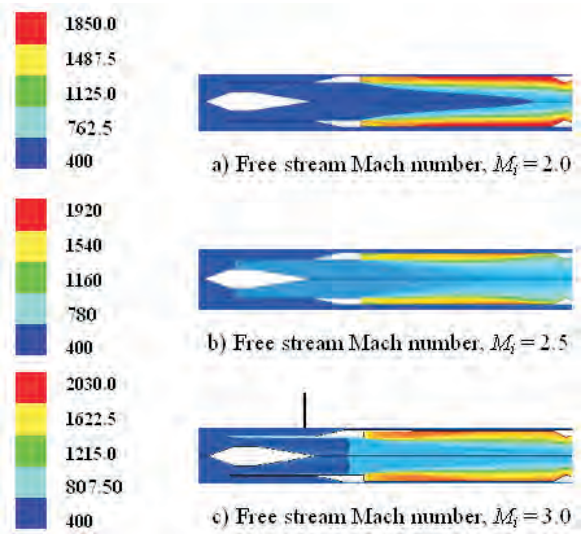

Figure 20. Temperature (K) contours for air/fuel ratio= 30.

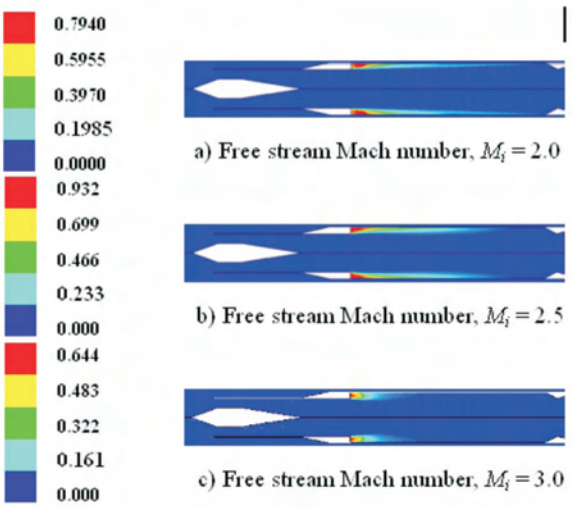

Figure 21. Mass fraction contours of fuel for air/fuel ratio= 30.

an A/F of 30. As a result of changes in the flow structure and air flow rate, combustion is poorer near the axis for A/F = 30. Thus, it is evident that the air fuel ratio plays a crucial role for the proper operation of a ramjet engine.

6. CONCLUSIONS

The overall performance of an integrated ramjet engine comprising of air-intake, combustor and nozzle has been investigated through full engine simulation. The coupled analysis clearly brings

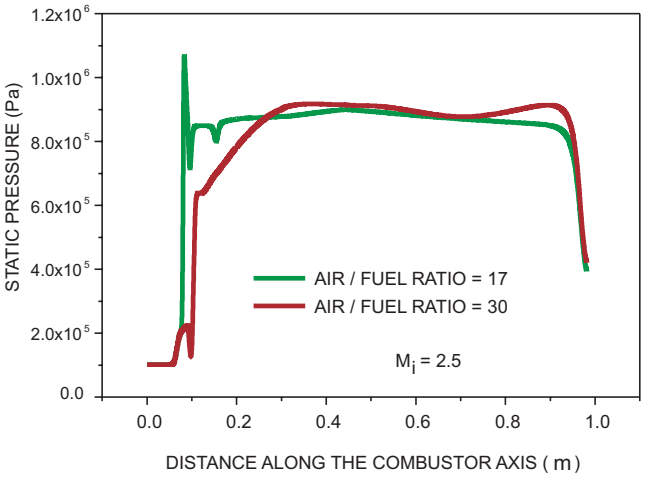

Figure 22. Variation of static pressure along the surface and axis of the centre body.

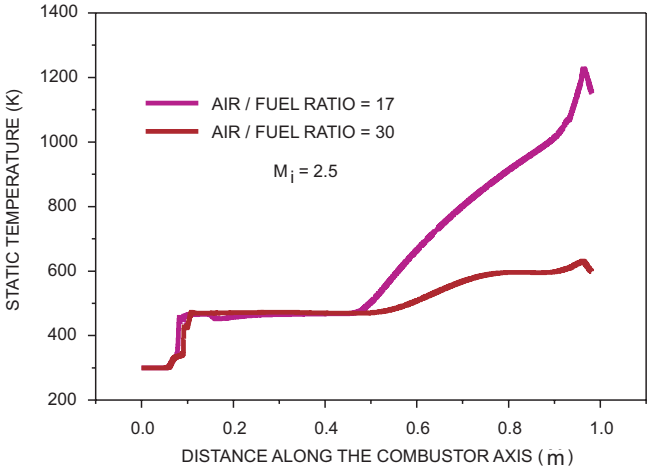

Figure 23. Variation of static temperature along surface and axis of the centre.

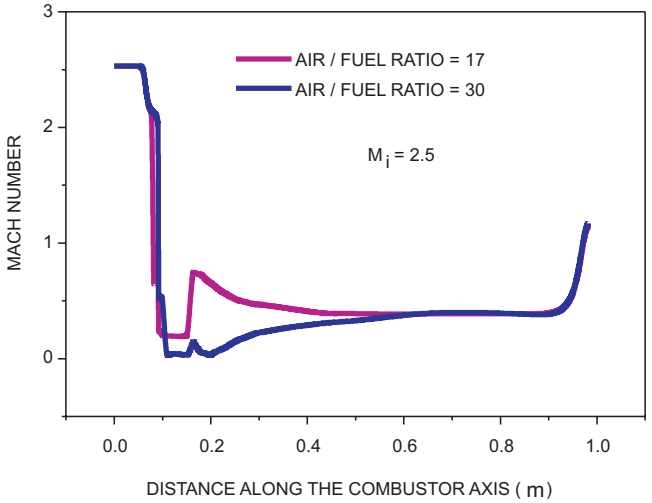

Figure 24. Mach number variation along the surface and axis of the centre body.

out the interaction between the air-intake and combustor. The air-intake performance is not only affected by its geometry but also by the amount of heat release in the combustor. The flow model developed in the present study has the potential to be used as a design and development tool in liquid fuelled ramjet development programmes.

ACKNOWLEDGEMENTS

The authors are extremely thankful to Shri P. Venugopalan, Director; and Dr S. Sundarrajan, Head, Programme Team, PJ-10, Defence Research and Development Laboratory (DRDL), Hyderabad, for their constant encouragement to complete this work successfully.

REFERENCES

1. Thomas, Jr. & A.N. Exploding ramjet myths. *National Defense,* 1983, 18-23.

2. Hebrard, P; Lavergne, G. & Torque, A. Ramjet and ramrocket performances: Experimental simulation and prediction by computation codes. *In* 10th ISOABE Proceedings, UK, 1991. pp. 1051-059. 1991. ISABE 91 - 7112.

3. Calzone ,R.F. Developments in missile Ramjet propulsion. TNO report. PML 1996 - A100.1991.

4. Cazin, P. & Laurent, J.M. Liquid-fuelled ramjet engine tactical missile propulsion. *Prog. Astro. Aero.*, 1996, **170**, 423-46.

5. Conway, S. & Johansson, J. Integrated engine-airframe calculations using CFD. 2001. AIAA Paper No. 2001-3201.

6. Sung, H.G.; Hsieh, S.Y. & Yang, V. A unified analysis of Ramjet operation in an integrated rocket ramjet engine. Part II Combustion dynamics of ramjet engine. AIAA Paper No. 2001-3192.

7. Gaiddon, A. & Knight, D.D. Aerodynamic optimization of the aeropropulsive system of a ramjet powered missile. 2002. AIAA Paper No. 2002-5546.

8. Launder, B.E. & Spalding, D.B. The numerical computation of turbulent flows. *Computer Methods Appl. Mech. Engg.,* 1974, **3**, 269-89.

9. Sreenatha, A.G. & Bhardwaj, N. Mach number controller for a flight vehicle with ramjet propulsion. 1999. AIAA Paper No. 99-2941 IP.

10. Mathew, G.; Lazar, T.C.; Debasis, C.; Paul, P.J. & Mukunda, H.S. Computational studies on the flow field in an ejector ramjet engine. Paper presented at National Conference on Air Breathing Engines and Aerospace Propulsion, Hyderabad, 1999, pp. 364-74.

11. Minard, J.P.; Hallais, M. & Falempin, F. Low cost ramjet technology for tactical missile application. AIAA Paper No. 2002 - 3765. *In* 38th AIAA/ASME/SAE/ASEE Joint Propulsion Conference & Exhibit, Indianapolis, Indiana. 2002.

Contributors

Dr G. Raja Singh Thangadurai obtained his ME (Aero Engg) and PhD (Mech Engg) from the Indian Institute of Science (IISc), Bangalore, in 1991 and the Indian Institute of Technology (IIT) Madras, Chennai, in 2004, respectively. Presently, he is working as Scientist E at the Defence Research & Development Laboratory (DRDL), Hyderabad. He is involved in the development of liquid propellant rocket engines and reaction control systems for *Prithvi* and *Agni* missiles. His areas of research are rocket and ramjet propulsion, numerical simulation of internal flows, and supersonic air intakes. He has contributed 10 papers in national journals and conferences.

Dr B.S. Subhash Chandran obtained his PhD (Aero Engg) from the Georgia Tech, USA, in 1984. Presently, he is working as Scientist at the DRDL, Hyderabad. He is actively engaged in the development of *Akash* propulsion system and liquid fuel ramjet engine for flight vehicles. His areas of interest are rocket and ramjet propulsion and supersonic air intakes. He has published 15 papers in national and international conferences.

Dr V. Babu obtained his PhD (Mech) from the Ohio State University, USA, in 1991. Presently, he is working as Associate Professor at the IIT Madras. His areas of research include: Computational simulation of internal/external flows, simulation of chemically reacting , plasma and nonequilibrium flows, high performance computing and development of software tools for engineering analysis. He is recipient of *Henry Ford Technology Award* (1998) presented by the Ford Motor Co, UK. for the design, development and deployment of a virtual aerodynamic/aero-acoustic wind tunnel. He has four patents to his credit.

Prof T. Sundararajan obtained his PhD (Mech Engg) from the University of Philadelphia, USA, in 1983. He worked as a postdoctoral fellow at the Univerity of Philadelphia, USA, from 1983-84. He joined as Assistant Professor at the IIT, Kanpur, in 1985. Presently, he is working at the IIT Madras, as Professor. He has guided 17 students for their PhD and 24 students for their MS. He has published 76 research papers in various journals and presented 85 papers in various conferences. He has also published a textbook on computational fluid dynamics. His areas of research include: Spray combustion, jet flows, heat transfer and fluid flow in porous media, and thermal modelling of manufacturing and metallurgical problems.